Comparison of Three Soot Models Applied to Multi-Dimensional Diesel Combustion Simulations*

Feng TAO**, Sukhin SRINIVAS**, Rolf D. REITZ** and David E. FOSTER**

In this paper, three soot models previously proposed for diesel combustion and soot formation studies are briefly reviewed and compared. The three models are (1) two-step empirical soot model, (2) eight-step phenomenological soot model, and (3) complex-chemistry coupled phenomenological soot model. All three models have been implemented into the KIVA-3V simulation code. For comparison, a heavy-duty DI diesel engine case with fuel injection typical of standard DI diesel operating conditions was studied. Flame structures of a single diesel spray predicted using these three models were compared, and the results offer our perspective on the application of these three models to soot modeling in diesel engines.

***Key Words*:** Soot Model, Diesel Spray, Flame Structure, Multi-Dimensional Simulation

1. Introduction

Multi-dimensional simulation has become an essential analysis tool in modern engine research and development. Recent practice of integrating multi-dimensional CFD with genetic algorithms (GAs)[1] has made simulation a possible design tool for exploring system optimization and control strategies of diesel engines. In the framework of the GA methodology, the merit value of an objective function of performance parameters (i.e., for example, soot, NOx, CO, HC and BSFC, etc.), which are subject to certain physical constraints, is evaluated from the simulations. It is therefore crucial to have an accurate prediction of soot formation, as well as other emissions and performance parameters in the objective function.

Indeed, modeling the soot formation process remains a key topic in studies of diesel engine combustion. Since the early 1970s when Khan et al.[2] first presented a model for the prediction of soot production from diesel engines, a variety of soot models with different levels of complexity have been proposed and applied to multi-dimensional simulations. In order to minimize engine-out soot emissions, to explore advanced engine operation modes and, in turn, to guide modern engine design and development, it is important that accurate and realistic soot models be used in multi-dimensional diesel simulations in order to provide reliable predictions of soot formation.

In this paper, we will briefly review soot formation models that have been proposed for studies of diesel engine combustion. Using a heavy-duty diesel engine case with fuel injection typical of standard DI diesel operating conditions, we compare three different modeling approaches, ranging in complexity from very simple to relatively detailed models. With more detailed models, we can obtain more valuable insights into the soot formation process, including information about soot particle size and soot number density distributions.

2. Model Review

2.1 Two-step empirical soot model

In the invited lecture at the first COMODIA conference in Tokyo in 1985, Hiroyasu[3] reviewed the soot models that had been published between 1962 and 1984. Among those, the two-step empirical soot model of Hiroyasu, Kadota and Arai[4] is the most well known. In their two-step model, Hiroyasu et al.[4] considered the soot formation process as involving only two reaction steps: (1) the formation step, in which soot is linked directly to fuel vapor molecules, and (2) the oxidation step, which describes the destruction of soot particles via the attack of molecular oxygen.

The net rate of change in soot mass is the difference between the rates of soot formation and oxidation, viz.,

$$\frac{dm_{soot}}{dt} = \left.\frac{dm_{soot}}{dt}\right|_{\text{form}} - \left.\frac{dm_{soot}}{dt}\right|_{\text{oxid}}, \qquad (1)$$

where the soot formation and oxidation rates are expressed in Arrhenius form as follows:

* Received 2nd May, 2005 (No. 05-5044)

** Engine Research Center, University of Wisconsin – Madison Madison, WI 53706, U.S.A.
E-mail: ftao@wisc.edu; reitz@engr.wisc.edu; foster@engr.wisc.edu

$$\left.\frac{dm_{soot}}{dt}\right|_{\text{form}} = A_f m_{fuel} p^{0.5} \exp\left(-\frac{E_f}{RT}\right) \quad (2)$$

$$\left.\frac{dm_{soot}}{dt}\right|_{\text{oxid}} = A_O m_{soot} X_{O_2} p^{1.8} \exp\left(-\frac{E_O}{RT}\right) \quad (3)$$

In Eqs. (2) and (3), m_{soot}, m_{fuel}, X_{O_2} and p are the soot mass, the fuel vapor mass, the oxygen molar fraction, and the pressure, respectively. The activation energies $E_f = 8\times10^4$ [J/mol] and $E_O = 12\times10^4$ [J/mol] were used[4]. The pre-exponential factors, A_f and A_O, are adjustable, and are determined by matching the calculated soot yields with measured data of soot production in the engine exhaust[4].

However, Patterson et al.[5] pointed out that Hiroyasu et al.'s soot model[4] or its revisions, for example, by Belardini et al.[6] under-predicted the peak in-cylinder soot concentration. Instead of using the original Hiroyasu et al's model, Patterson et al. adopted the value of the activation energy $E_f = 5.25\times10^4$ [J/mol] proposed by Belardini et al.[6] for the soot formation step, and replaced the soot oxidation formulation by the Nagle and Strickland-Constable (*NSC*) oxidation model[7].

The *NSC* oxidation reactions are semi-empirical, involving two reaction sites on the surface of a soot particle: (1) significantly more reactive sites A and (2) less reactive sites B. The fraction of the surface site A is denoted by x_A, and the remaining fraction $1-x_A$ is for the surface site B. The *NSC* reaction scheme can be described as follows:

$A_{\text{site}} + O_2(g) \xrightarrow{k_A}$ Surface Oxide :

$$k_A = 20\exp(-15\,100/T)\ [\text{g/cm}^2\ \text{s atm}] \quad (4)$$

Surface Oxide $\xrightarrow{k_A/k_Z}$ 2CO(g) + A_{site} :

$$k_Z = 21.3\exp(2\,060/T)\ [\text{atm}^{-1}] \quad (5)$$

$B_{\text{site}} + O_2(g) \xrightarrow{k_B}$ 2CO(g) + A_{site} :

$$k_B = 4.46\times10^{-3}\exp(-7\,640/T)\ [\text{g/cm}^2\ \text{s atm}] \quad (6)$$

$A_{\text{site}} \xrightarrow{k_T} B_{\text{site}}$:

$$k_T = 1.51\times10^5\exp(-48\,800/T)\ [\text{g/cm}^2\ \text{s}] \quad (7)$$

The *NSC* oxidation rate (units of mole C-atom/cm^2 s) is given by:

$$\dot{R}_{NSC} = \left[\left(\frac{k_A p_{O2}}{1+k_Z p_{O2}}\right)x_A + k_B p_{O2}(1-x_A)\right], \quad (8)$$

where the fraction x_A can be calculated by the steady-state assumption of site A formation:

$$x_A = (1 + k_T/k_B p_{O2})^{-1} \quad (9)$$

The oxidation rate of soot mass related to the *NSC* model is determined by:

$$\left.\frac{dm_{soot}}{dt}\right|_{\text{oxid}} = \frac{6m_{soot}}{\rho_{soot} D_{soot}} M_C \dot{R}_{NSC} \quad (10)$$

where M_C, ρ_{soot}, and D_{soot} are the molecular weight of a carbon atom (12.011 g/mole), the soot particle density (2 g/cm^3), and the diameter of a soot particle (25 nm), respectively.

Due to its simplicity, this modified version of the two-step soot model[5] has acquired wide popularity in the community engaged in multi-dimensional diesel engine simulations.

2.2 Eight-step phenomenological soot model

At the third COMODIA conference in Yokohama in 1994, Fusco, Knox-Kelecy and Foster[8] proposed an eight-step phenomenological soot model for diesel studies. Like many others[9]–[14], Fusco et al.[8] questioned the applicability of the two-step empirical models when applied over a wide range of conditions in diesel engine simulations, and suggested to relax the strong tie between fuel vapor molecules and soot by introducing two intermediate species. The eight global reaction steps include particle inception, particle coagulation, surface growth, and surface oxidation, as well as global reaction steps for intermediate species formation and oxidation (see the schematic in Fig. 1):

$Fuel \xrightarrow{k_1} \upsilon_1 R$:

$$k_1 = 0.7\times10^{12}\exp\left(-1.2\times10^5/RT\right) \quad (11)$$

$Fuel \xrightarrow{k_2} \upsilon_2 C_2H_2$:

$$k_2 = 2.0\times10^8\exp\left(-4.9\times10^4/RT\right) \quad (12)$$

$R + O_2 \xrightarrow{k_3}$ Product :

$$k_3 = 1.0\times10^{12}\exp\left(-4.0\times10^4/RT\right) \quad (13)$$

$C_2H_2 + O_2 \xrightarrow{k_4} 2CO + H_2$:

$$k_4 = 6.0\times10^{13}\exp\left(-5.0\times10^4/RT\right) \quad (14)$$

$R \xrightarrow{k_5} C_{soot}$:

$$k_5 = 1.0\times10^{10}\exp\left(-5.0\times10^4/RT\right) \quad (15)$$

$C_{soot} + C_2H_2 \xrightarrow{k_6} C_{soot+2} + H_2$:

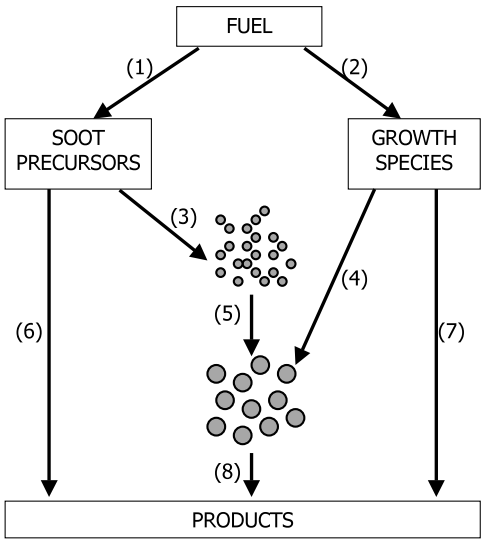

Fig. 1 Schematic of eight-step phenomenological soot model (reproduced from Fusco et al.[8])

$$k_6 = 4.2\times10^4 \exp\left(-1.2\times10^4/RT\right) \quad (16)$$

$$C_{soot} + O_2 \xrightarrow{\dot{R}_7} C_{soot} + 2CO:$$

$$\dot{R}_7 = \dot{R}_{NSC} \quad (17)$$

$$xC_{soot} \xrightarrow{k_8} C_{soot}:$$

$$k_8 = 1.05\times10^{-7} \quad (18)$$

The net rates of formation for the precursor species, R, acetylene, C_2H_2, the soot volume fraction, f_V, and the soot number density, f_N, can be written as:

$$\frac{d}{dt}[R] = \upsilon_1 k_1[Fuel] - k_3[R][O_2] - k_5[R] \quad (19)$$

$$\frac{d}{dt}[C_2H_2] = \upsilon_2 k_2[Fuel] - k_4[C_2H_2][O_2] - k_6[C_2H_2](A_{soot})^{1/2} \quad (20)$$

$$\frac{d}{dt}(\rho_s f_V) = \left(k_5[R] + k_6[C_2H_2](A_{soot})^{1/2} - \frac{6m_{soot}}{\rho_{soot}D_{soot}}\dot{R}_{NSC}\right)M_C \quad (21)$$

$$\frac{d}{dt}(f_N/N_A) = k_5[R] - k_8 T^{1/2}(f_v)^{1/6}(f_N)^{11/6} \quad (22)$$

Here, υ_1, υ_2 are the stoichiometric coefficients, [ ] indicates the molar concentration (units of mole/cm^3), $A_{Soot} = \pi(D_{Soot})^2 f_N$ is the total soot surface area density (units of cm^2/cm^3), and N_A is Avogadro's number.

Fusco et al.[8] considered in their model a generic soot radical precursor and specified acetylene to be the soot growth species. However, as coupling of large-scale chemical kinetic mechanisms with CFD codes for multi-dimensional engine simulations was not pursued at the time, they assumed the soot precursor radical and the soot growth species to be the products of pure fuel pyrolysis, each of which was represented only by one global reaction step. Later, aiming at a better description of the particle physics of soot formation, Kazakov and Foster[15] suggested using a generic species for the soot surface growth and a rate constant of coagulation that is valid from the molecular to the continuum regimes. In this manner, the description of the soot formation process becomes more physically sound, compared to the two-step empirical model and, yet, this model retains its simplicity. Fusco et al.'s model is continuously receiving renewed attention[16),(17)].

2.3 Complex-chemistry coupled phenomenological soot model

Tao, Golovitchev and Chomiak[18] presented a paper at the fifth COMODIA in Nagoya in 2001. In the paper, a chemical mechanism that couples a phenomenological soot model with complex chemistry for gas-phase soot precursor formation and oxidation was described. This mechanism consists of 65 species and 268 reac-

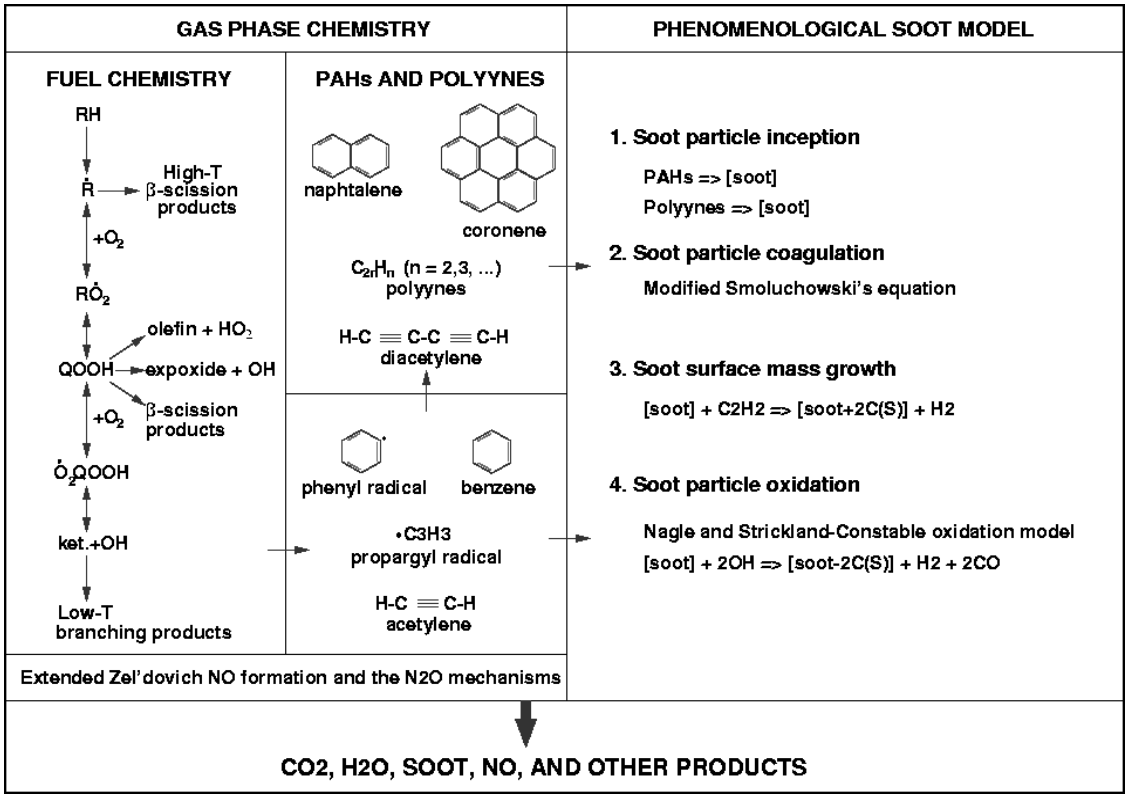

Fig. 2 Modular structure of the chemical mechanism coupling the phenomenological soot model with detailed gas-phase chemistry (reproduced from Tao et al.[19])

Table 1 Engine specification and operating conditions

Engine	Caterpillar 3401E SCOTE
Bore	137.2 mm
Stroke	165.1 mm
Compression ratio	16.1:1
Displacement	2.44 Liters
Connecting rod length	261.6 mm
Squish height	1.57 mm
Combustion chamber geometry	In-Piston Mexican Hat with Sharp Edged Crater
Piston	Articulated
Charge Mixture Motion	Quiescent
Maximum Injection Pressure	190 Mpa
Injector type	A production style Caterpillar electronic unit injector (EUI)
Number of Nozzle holes	6
Nozzle Hole Diameter	0.214 mm
Injector position from the head	2.05 mm
Speed	821 rpm
Load	25%
SOI	-10 degree ATDC
EGR	7.79

tions, and was incorporated into KIVA CFD calculations for the study of the detailed flame structure of diesel sprays[18]–[20].

The modular structure of the mechanism[18] is illustrated in Fig. 2. The idea of constructing this mechanism followed the same reasoning as for the eight-step phenomenological model of Fusco et al.[8] and Kazakov et al.[15] Instead of using global reaction steps for acetylene and precursor formation, the mechanism includes detailed chemical reactions for the formation of poly aromatic hydrocarbons (PAHs) and polyyne formation, both of which were considered to be possible precursors leading to soot particles. The PAH formation mechanism of Wang and Frenklach[21] was used to construct the formation reactions of higher, linear hydrocarbons (up to C6 species), and the formation of benzene and further reactions leading to naphthalene. The soot formation model includes the following important steps: particle inception, in which naphtalene (A_2) and diacetylene (C_4H_2) grow irreversibly to form soot; surface growth via the addition of acetylene (C_2H_2); surface oxidation via OH and O_2 attack. This soot formation mechanism is combined with n-heptane ignition chemistry and small hydrocarbon oxidation chemistry, forming the main body of the mechanism. The full listing of the mechanism is provided elsewhere[20].

3. Engine Experiments

A series of experiments on a Caterpillar 3401E single cylinder oil test engine have been performed at Engine Research Center (ERC), University of Wisconsin–Madison. The engine specifications and operating conditions are listed in Table 1. Kong et al.[22] have carried out numerical simulations to validate many test cases, and thus we do not repeat the same validation work in this paper. We choose one of the cases (Case B2 in Table 3 of Ref. (22)) and compare the predicted results using different soot modeling approaches. To make the phasing of the predicted cylinder pressure traces agree with the experimental data, the parameters important for ignition

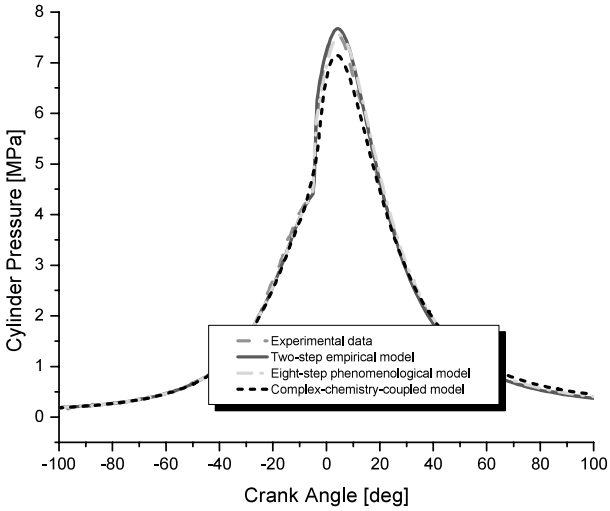

Fig. 3 Comparison of in-cylinder pressure traces between the measured data and the predicted results using three different soot modeling approaches

were adjusted for the three modeling approaches. The in-cylinder pressures from the predictions and the experiment agree very well, as shown in Fig. 3.

4. Results and Discussion

4.1 Experimental background

In the following comparisons, we illustrate the predicted spatial distributions of combustion and soot using three different soot modeling approaches and discuss the differences. However, as there were no direct imaging measurements from the experiments of Caterpillar 3401E engine, Dec's diesel conceptual model[23] is referred to as a guideline.

In the conceptual model (see Fig. 4), Dec summarized the work carried out by his research group using a variety of laser diagnostic methodologies on the combustion of a diesel fuel jet in a quiescent heavy-duty diesel engine, and depicted an idealized schematic of a reacting diesel fuel jet during the quasi-steady period, i.e. the period after the initial premixed burn until the wall impingement of the reacting jet. Dec characterized the structure of the free reacting jet as consisting of a very rich premixed reaction zone, which leads to the initial soot formation, followed by a soot-filled central region that is surrounded by a diffusion flame. The diffusion flame is lifted a certain distance downstream from the nozzle tip. The fuel vapor does not penetrate too far to form the rich premixed zone. As long as the diffusion flame remains intact, the soot particles travel down the jet along with the other rich products and burn out at the near-stoichiometric diffusion flame.

4.2 Two-step empirical soot model

The modified version of two-step soot model proposed by Patterson et al.[5] was used for the present simulations. The model has been implemented into the standard ERC KIVA-3V code, which features the "Shell"

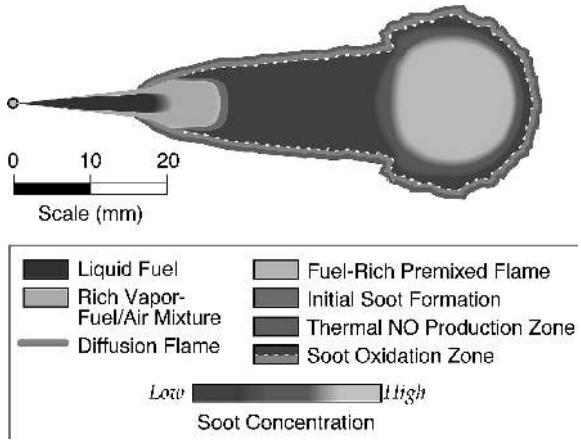

Fig. 4 Schematic of Dec's conceptual diesel model, showing the main features of a reacting diesel fuel jet during the quasi-steady portion of combustion (reproduced from Dec[23])

model for ignition, Zel'dovich model for NO formation, a wave model for spray breakup, and a crevice model for piston-ring flow, etc. More details of model improvements are described in Ref. (22).

Figure 5 illustrates spatial distributions of temperature, soot mass, fuel vapor, oxygen, NO and the main combustion products (carbon dioxide, water, carbon monoxide) at the end of injection (−2.5 °CA ATDC). The simulation predicts a flame that starts close to the nozzle tip. CO_2 and H_2O are mainly formed along the flame surface. Inside the flame region, equivalence ratio is high due to high fuel concentration and large depletion of O_2, where substantial CO is formed. The predicted peak NO concentration region coincides with the location of highest temperature, as expected.

Although the simulation did not predict a lifted flame in this case, the spatial soot distribution seems reasonable, i.e., highly concentrated soot is located inside the leading part of the rich combustion zone. In Fig. 5, the soot formation can be easily correlated with the soot precursor (fuel vapor in this case) and with the oxidant (molecular oxygen). The fuel vapor extends from injector to the piston bowl, and oxygen is highly depleted inside the flame. Thus, soot formation is strongly favored and soot is predicted starting close to the nozzle tip, which is inconsistent with Dec's observation.

4.3 Eight-step phenomenological soot model

The eight-step soot model of Fusco et al.[8] was implemented in the same KIVA-3V code as for the previous simulation. The predicted temperature, fuel vapor, oxygen, NO, as well as soot relevant quantities (soot mass, soot precursor, acetylene, and soot number density) distributions are illustrated in Fig. 6. The distributions of the main combustion products (carbon dioxide, water, carbon monoxide) are similar to those predicted previously and thus are not shown in Fig. 6.

Comparing the predicted soot distribution in Fig. 6 with that in Fig. 5, we see noticeable differences. In this simulation, soot is formed mainly in the leading part of the flame and its distribution does not extend upstream to nozzle tip. The temperature close to the nozzle is relatively low and soot formation is suppressed. This feature is consistent with Dec's conceptual model. The predicted soot precursor and acetylene distributions seem also to agree with Dec's description on the sequences of soot formation process, i.e., following the fuel injection direction, a high concentration of soot precursors that contributes to soot inception is formed prior to the soot cloud; in the region where the soot cloud is located, a high concentration of acetylene exists, contributing to soot mass buildup via surface growth. The improvement of soot formation prediction can be attributed to the different approach used by the eight-step soot model, where a soot precursor and a growth species (acetylene) are considered, instead of just fuel vapor as used in two-step soot model.

4.4 Complex-chemistry coupled phenomenological soot model

The phenomenological soot model coupled with complex chemistry mechanism was incorporated into the KIVA-3V (Rel.2) code. The crevice model that was used in the previous simulations was also implemented in the code. To handle the turbulence-chemistry interaction, a "subgrid" partially stirred reactor model was applied[19),(20)].

Figure 7 illustrates the spatial distributions of temperature, fuel vapor, molecular oxygen, NO, soot mass, soot precursors (diacetylene C_4H_2 and naphthalene A_2), and soot growth species (acetylene C_2H_2) at the end of injection. While the major features of the flame are similar to those of the previous two predictions, a noticeable difference is that the predicted diffusion flame is lifted from the nozzle tip, as indicated by the location of the high temperature region close to the nozzle. This feature has been observed in many experimental studies, such as those of Dec and coworkers[23].

Other interesting features are that the predicted fuel vapor penetration is not as far as predicted with simpler combustion model; the oxygen concentration near the nozzle tip is not depleted. This oxygen distribution indicates air entrainment upstream of the flame liftoff region, which is again consistent with Dec's conceptual model.

The soot spatial distribution also agrees well with the description in Dec's conceptual model. Figure 7 shows that soot begins to form near the tip of the fuel plume, where the premixed portion of combustion dominates. The soot concentration is high downstream inside the rich combustion zone but gradually burns out towards the flame. Examining the distributions of soot precursors and growth species in Fig. 7 suggests that polyynes play a stronger role in the soot formation process than PAHs in

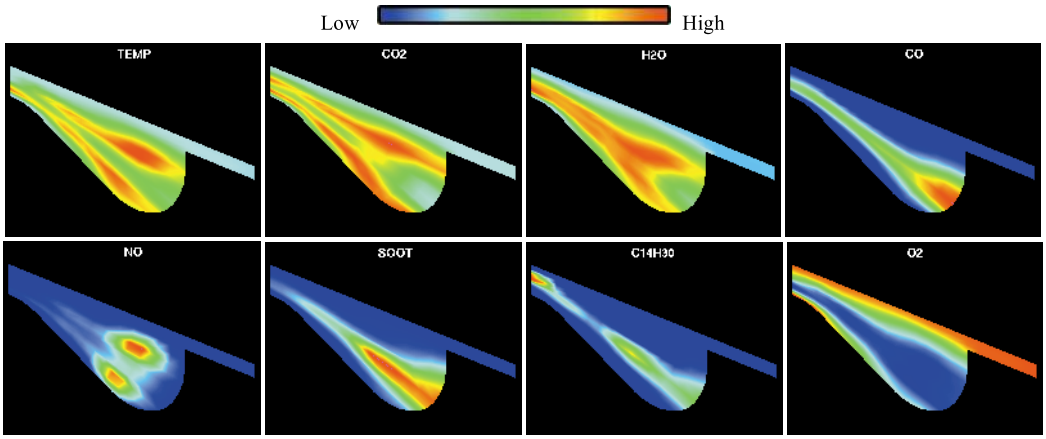

Fig. 5 Spatial distributions of temperature, carbon dioxide (CO_2), water (H_2O), carbon monoxide (CO), NO, soot mass, fuel vapor, and molecular oxygen (O_2) at the end of injection. The blue color indicates the low end of the legend and the red color for the high end of the legend: temperature (500 – 2 500 K), CO_2 (0 – 1 200 g/m^3), H_2O (0 – 700 g/m^3), CO (0 – 3 200 g/m^3), NO (0 – 10 g/m^3), soot (0 – 12 g/m^3), $C_{14}H_{30}$ (0 – 3 000 g/m^3), and O_2 (0 – 5 300 g/m^3)

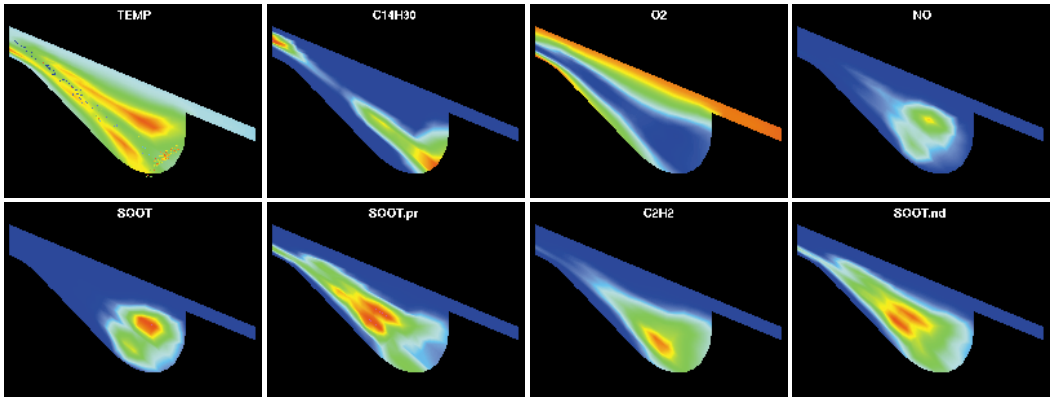

Fig. 6 Spatial distributions of temperature, fuel vapor, molecular oxygen (O_2), NO, soot mass, soot precursor, soot growth species (acetylene C_2H_2) and soot number density at the end of injection. The blue color indicates the low end of the legend and the red color for the high end of the legend: temperature (500 – 2 500 K), $C_{14}H_{30}$ (0 – 3 000 g/m^3), O_2 (0 – 5 300 g/m^3), NO (0 – 10 g/m^3), soot (0 – 12 g/m^3), soot precursor (0 – 0.015 g/m^3), C_2H_2 (0 – 80 g/m^3), and soot number density (0 – 6×10^{16} particles/m^3)

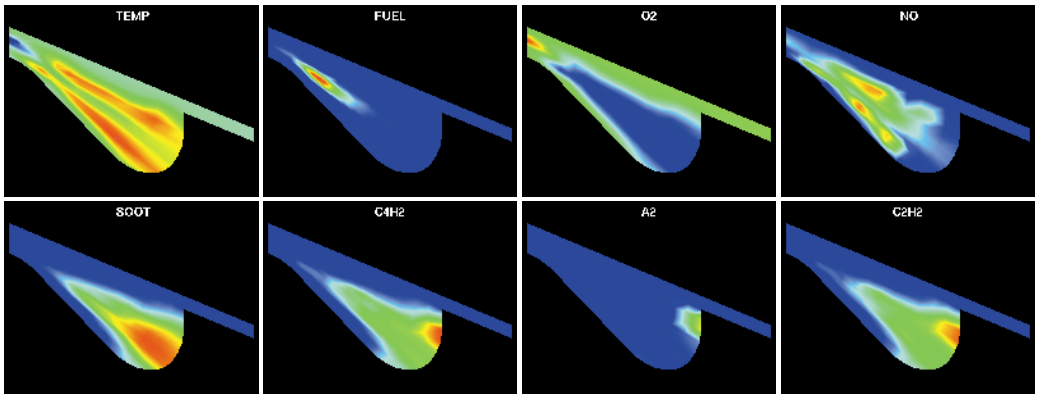

Fig. 7 Spatial distributions of temperature, fuel vapor, molecular oxygen, NO, soot mass, soot precursors (C_4H_2 and A_2), soot growth species (acetylene C_2H_2) at the end of injection. The blue color indicates the low end of the legend and the red color for the high end of the legend: temperature (500 – 2 000 K), Fuel (0 – 3 000 g/m^3), O_2 (0 – 5 300 g/m^3), NO (0 – 10 g/m^3), soot (0 – 12 g/m^3), soot precursor (0 – 0.015 g/m^3), C_2H_2 (0 – 80 g/m^3), and soot number density (0 – 6×10^{16} particles/m^3)

this case. The present simulation indicates that further experimental studies are needed to verify the important soot formation steps predicted by the model. The prediction of NO formation is in agreement and is consistent with Dec's conceptual model as well.

5. Conclusion

In this paper, three soot models that have been proposed for multi-dimensional diesel engine simulations are reviewed. By applying these three different models to the same test case of a heavy-duty diesel engine with fuel injection typical of standard DI diesel operating conditions, important differences between the predictions are revealed.

(1) The two-step empirical soot model is ease to be implemented into CFD codes and to be adjusted for matching the predictions with measurements. The simulation can capture the main features of flame and soot distributions of diesel sprays in engines, but the present results show that the predicted flame in the near-nozzle region does not agree well with the diesel flame structure of Dec[23]. The detailed information of soot formation cannot be obtained using this modeling approach.

(2) The eight-step soot phenomenological model shares similar advantages to the two-step model and, besides, it is very computationally efficient. The simulations using the eight-step model can predict the same flame structure of diesel sprays as that of using the two-step soot model. The prediction of soot distribution is improved and, additionally, the simulations provide more useful information such as soot precursor, acetylene, soot number density as well as soot particle size. Compared to the previous model, the eight-step model offers better description of physics of soot formation. However, the parameters of the rate constants leading to soot precursor, soot particles and soot surface growth require a little more tuning work. Recently, further improvement of the phenomenological soot model was pursued and its application to high-speed direct injection (HSDI) diesel engines[24),(25)] leads to some new insights in low-temperature diesel combustion.

(3) The implementation of complex-chemistry and phenomenological soot model into multi-dimensional CFD codes offer many advantages for the prediction of the diesel flame structure over the previous two models. The prediction shows that the flame of diesel sprays injected at standard DI operating conditions is lifted from nozzle tip, allowing substantial oxygen to be entrained into the core region of the spray jet. This predicted flame structure, as well as the predicted fuel vapor penetration, soot and NO distributions, agrees well with that of Dec[23]. The simulations provide also very detailed information of many other species such as naphthalene and diacetylene, all of which are important agents in the soot formation process. However, the complexity of the chemical mechanism introduces many uncertainties and increases significantly computational times.

Acknowledgements

This work was supported by Caterpillar Inc. and by the Ford Research Center in Aachen-Germany (FFA). The authors appreciate gratefully Dr. Song-Chang Kong for providing the experimental data and Dr. Randy Hessel for his help during the simulations.

References

(1) Senecal, P.K., Montgomery, D.T. and Reitz, R.D., A Methodology for Engine Design Using Multi-Dimensional Modeling and Genetic Algorithms with Validation through Experiments, International Journal of Engine Research, Vol.1 (2000), pp.229–248.

(2) Khan, I.M., Greeves, G. and Wang, C.H.T., Factors Affecting Smoke and Gaseous Emissions from Direct Injection Engines and a Method of Calculation, SAE Paper 730169, (1973).

(3) Hiroyasu, H., Diesel Engine Combustion and Its Modeling, COMODIA 85 (1985), pp.53–75.

(4) Hiroyasu, H., Kadota, T. and Arai, M., Development and Use of a Spray Combustion Modeling to Predict Diesel Engine Efficiency and Pollutant Emissions (Part I: Combustion Modeling), Bulletin of the JSME, Vol.26 (1983) pp.569–575.

(5) Patterson, M., Kong, S.-C., Hampson, G. and Reitz, R.D., Modeling the Effects of Fuel Injection Characteristics on Diesel Engine Soot and NOx Emissions, SAE Paper 940523, (1994).

(6) Belardini, P., Bertoli, C., Ciajolo, A., D'Anna, A. and Del Giacomo, N., Three-Dimensional Calculations of DI Diesel Engine Combustion and Comparison with In-Cylinder Sampling Valve Data, SAE Paper 922225, (1992).

(7) Nagle, J. and Strickland-Constable, R.F., Oxidation of Carbon between 1000–2000°C, Proceedings of the Fifth Carbon Conference, Part 1 (1962), pp.265–325.

(8) Fusco, A., Knox-Kelecy, A.L. and Foster, D.E., Application of a Phenomenological Soot Model for Diesel Engine Combustion, COMODIA 94 (1994), pp.571–576.

(9) Leung, K.M., Lindstedt, R.P. and Jones, W.P., A Simplified Reaction Mechanism of Soot Formation in Non-Premixed Flames, Combust. Flame, Vol.87 (1991), pp.289–305.

(10) Zellat, M., Rolland, Th. and Poplow, F., Three-Dimensional Modeling of Combustion and Soot Formation in an Indirect Injection Diesel Engines, SAE Paper 900254, (1990).

(11) Nakakita, K., Nagaoka, M., Fujikawa, T., Ohsawa, K. and Yamaguchi, S., Photographic and Three-Dimensional Numerical Studies of Diesel Soot Formation Process, SAE Paper 902081, (1990).

(12) Gorokhovski, M. and Borghi, R., Numerical Simulation of Soot Formation and Oxidation in Diesel Engines, SAE Paper 930075, (1993).

(13) Belardini, P., Bertoli, C., Del Giacomo, N. and Iorio,

B., Soot Formation and Oxidation in a DI Diesel Engine: A Comparison between Measurements and Three-Dimensional Computations, SAE Paper 932658, (1993).

(14) Belardini, P., Bertoli, C., Beatrice, C., D'Anna, A. and Del Giacomo, N., Application of a Reduced Kinetic Model for Soot Formation and Burnout in Three-Dimensional Diesel Combustion Computations, Proc. Combust. Inst., Vol.26 (1996), pp.2517–2524.

(15) Kazakov, A. and Foster, D.E., Modeling of Soot Formation during DI Diesel Combustion Using a Multi-Step Phenomenological Model, SAE Paper 982463, (1998).

(16) Ishii, H., Goto, Y., Odaka, M., Kazakov, A. and Foster, D.E., Comparison of Numerical Results and Experimental Data on Emission Production Processes in a Diesel Engine, SAE Paper 2001-01-0656, (2001).

(17) Lee, S., Sung, N., Shin, D. and Lee, J., Soot Emission from a Direct Injection Diesel Engine, SAE Paper 2004-01-0927, (2004).

(18) Tao, F., Golovitchev, V.I. and Chomiak, J., Application of Complex Chemistry to Investigate Combustion Zone Structure of DI Diesel Sprays under Engine-Like Conditions, COMODIA 2001 (2001), pp.92–100.

(19) Tao, F. and Chomiak, J., Numerical Investigation of Reaction Zone Structure and Flame Liftoff of DI Diesel Sprays with Complex Chemistry, SAE Paper 2002-01-1114, (2002).

(20) Tao, F., Numerical Modeling of Soot and NOx Formation in Non-Stationary Diesel Flames with Complex Chemistry, Ph.D. Thesis, Chalmers University of Technology, (2003).

(21) Wang, H. and Frenklach, M., A Detailed Kinetic Modeling Study of Aromatics Formation in Laminar Premixed Acetylene and Ethylene Flames, Combust. Flame, Vol.110 (1997), pp.173–221.

(22) Kong, S.-C., Patel, A., Yin, Q., Klingbeil, A. and Reitz, R.D., Numerical Modeling of Diesel Engine Combustion and Emissions under HCCI-Like Conditions with High EGR Levels, SAE Paper 2003-01-1087, (2003).

(23) Dec, J.E., A Conceptual Model of DI Diesel Combustion Based on Laser-Sheet Imaging, SAE Paper 970873, (1997).

(24) Tao, F., Liu, Y., RempelEwert, B.A., Foster, D.E., Reitz, R.D., Choi, D. and Miles, P.C., Modeling the Effects of EGR and Injection Pressure on Soot Formation in a High-Speed Direct-Injection (HSDI) Diesel Engine Using a Multi-Step Phenomenological Soot Model, SAE Paper 2005-01-0121, (2005).

(25) Liu, Y., Tao, F., Foster, D.E. and Reitz, R.D., Application of an Improved Multiple-Step Phenomenological Soot Model to a HSDI Diesel Multiple Injection Modeling, SAE Paper 2005-01-0924, (2005).